ELSEVIER

PII: S0032-3861(97)00106-7

*Polymer* Vol. 38 No. 22, pp. 5643–5651, 1997

0032-3861/97/$17.00 + 0.00

# The structure and morphology of lamellar single crystals of PK99, with a note on melt growth rates

**Mariarosa Bellomo†, Lourdes Franco‡ and Mary Hill***
*H. H. Wills Physics Laboratory, University of Bristol, Tyndall Avenue, Bristol BS8 1TL, UK*
*(Received 29 March 1996; revised 7 October 1996)*

Lamellar single crystals of the aromatic polyketone PK99 have been grown from dilute solution in benzophenone. The crystals are multilayer and shaped like extended leaves, they then twist about their long axes. Selected area electron diffraction and wide angle X-ray diffraction (WAXD) of crystal mats show that the unit cell is orthorhombic with $a = 0.788$ nm, $b = 0.609$ nm and $c = 4.82$ nm. This structure is also found for the melt drawn fibre and is similar to that suggested by other authors who looked at melt crystallized material. The unit cell is slightly larger than the unit cells of PEEK and PEK in the $hk0$ plane. Small angle X-ray diffraction of solution grown crystals indicates a long period of 7.86 nm, this thickness is close to one and a half times the chain repeat. The growth rate from the melt has been investigated as a function of crystallization temperature, using both optical and transmission electron microscopy (TEM). Results from the two techniques agree within the experimental errors. As has been found by other authors, there is a maximum growth rate at 260°C, a minimum between 235 and 240°C and a second, much lower, maximum at 230°C. © 1997 Elsevier Science Ltd.

**(Keywords: PK99; solution crystallization; diffraction)**

## INTRODUCTION

In recent years polymers with aromatic backbones have become of general interest for their high melting points, thermal stability and good mechanical properties at elevated temperatures. PEEK is the best known of these materials, but others, with differing numbers of ketone and ether linkages, have also been synthesized[1]. One of the more recent materials is an aromatic polyketone designated PK99, a polymer with the chain structure shown in *Figure 1*. Because the aromatic units are not all linked in the *para* fashion, but the unit between carbonyl (C = O) groups is linked in the *meta* form (see *Figure 1*), the melting point is lowered so that processing is easier[2,3]. The melting point ($T_m$) of PK99 crystallized on slow cooling from the melt is 306°C[3] (compared with PEEK at 345°C and PEK at 367°C[4]). The glass transition temperature ($T_g$) of PK99 is 158°C, giving a favourable $T_g/T_m$ (K) ratio of 0.75 (compared with PEEK at 0.68). Thus PK99 shows promise of industrial usefulness.

PK99 is known to crystallize from the melt. The as-made material has 35% crystallinity[3] and although crystals do not form on cooling from the melt at 20°C min$^{-1}$ they develop on annealing at any temperature between 200 and 300°C[2]. An unusual double maximum has been observed for spherulitic growth rates, with a maximum rate at about 270°C, a minimum value at 245°C and a second (much lower) maximum at 230°C[2]. This double maximum in growth rate has been attributed[2,3] to a 'self poisoning' mechanism as a result of the interrelation of the chain sequence length with the crystal thickness, coupled with an energy penalty from inclusion of the *meta* unit in the crystal. (Self-poisoning mechanisms, but with different causes, have also been documented in alkane oligomers[5] and polyethylene oxide[6].) X-ray studies show that PK99 crystallized from the melt throughout the crystallization range has the same structure, but that the crystals are markedly thicker when crystallized from higher temperatures[2,3]. The unit cell of the melt crystallized material, deduced from X-ray diffraction by Blundell *et al.*[3], is orthorhombic with $a = 0.785$ nm, $b = 0.605$ nm and, along the chain direction, $c = 4.77$ nm. As Blundell remarks[7], the unit cells of the aryl-ether-ketone polymers, PEEK, PEK, PK99 and a number of others, are all orthorhombic and the $a/b$ projections are similar.

In this paper we describe the crystallization of PK99 from solution, as far as we know this has not been recorded elsewhere. However, other polyaryls have been crystallized from solution; both PEEK and PEK are soluble in benzophenone and crystallize from solution to give lamellar single crystals[4,8]. We have dissolved PK99 in benzophenone and crystallized to obtain lamellar single crystals. We have examined these crystals by TEM, using imaging and diffraction, and with wide and small angle X-rays. We have also obtained X-ray data from well oriented melt crystallized fibres. We have determined the crystal structure of PK99 from our diffraction data, finding the cell to be

* To whom correspondence should be addressed
† Present address: Intituto Chimico, Facoltà d'Ingegueria, Università di Catania, Viale A Doria 8, 95121 Catania, Italy
‡ Present address: Departament d'Enginyeria Quimica, E.T.S. d'Enginyers Industrials de Barcelona, Universitat Politecnica de Catalunya, E-08028 Barcelona, Spain

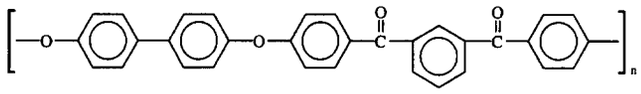

**Figure 1** Chemical repeat of PK99. This polymer incorporates both bi-phenyl and *meta*-phenyl units regularly spaced along the chain

orthorhombic with $a = 0.788$ nm, $b = 0.609$ nm and $c = 4.82$ nm. This cell is consistent with all our data; that obtained from electron diffraction of individual single crystal lamellae and from X-ray diffraction, both of single crystal mats and of melt drawn fibres. Note that our unit cell is very like that found by Blundell *et al.*[3] for melt crystallized PK99. In addition to our work with single crystals and fibres, we have used optical microscopy (OM) and TEM to measure the growth rates of spherulitic crystals, from the melt, at various temperatures.

## EXPERIMENTAL

The polymer PK99 was synthesized, at the University of Catania, Italy[9]. We found that PK99 dissolves in benzophenone when held at 260°C in a constant temperature oil bath. In order to produce crystals for TEM, 1 mg of the polymer was dissolved in 1 ml of solvent; 10 mg were dissolved in 15 ml to make a crystal mat for X-ray work. In both cases the solution was cooled to room temperature and the polymer crystallized during cooling. Benzophenone is solid at room temperature ($T_m$ 48°C) but the crystals can be extracted from the solid solvent by the addition of acetone, a solvent for benzophenone but not for the polymer. Thus, we obtained a suspension of crystals in acetone; the crystals were subsequently washed in *n*-butanol several times.

Crystals were mounted on carbon coated copper grids for examination in the TEM. Some crystals were shadowed with platinum palladium in order to calibrate the diffraction patterns and to make the real space images clearer. Other crystals were decorated with polyethylene vapour before shadowing, following the technique of Wittmann and Lotz[10]. We used a Philips 301 TEM, operated at 80 kV. Wide angle X-ray scattering (WAXS) was performed using a Philips PW 1729 X-ray generator fitted with an evacuated flat plate camera, and low angle X-ray pictures were taken using a Rigaku–Denki camera with specimen to film distance 29.3 cm. X-ray diffraction patterns were recorded under vacuum at room temperature. Calcite ($d_B = 0.3035$ nm) was dusted onto selected samples for calibration purposes.

Thin films, for optical microscopy, were melt pressed. These pressed films were subsequently melted for 10 min at 380°C in a Linkam hot stage and then cooled, at 50°C min$^{-1}$, to the required crystallization temperature. An Ultraphot optical microscope was used to observe crystallization for up to 30 min; pictures were taken at regular intervals using a Zeiss camera mounted on the microscope. Crystal growth rates were measured from these optical micrographs or from video recordings of the growth. Growth rates were measured at intervals of 5°C between 210 and 285°C. Optical microscopy was more difficult at the lowest temperatures because of the high nucleation density. TEM studies were undertaken to complement the OM, growth rates being measured at

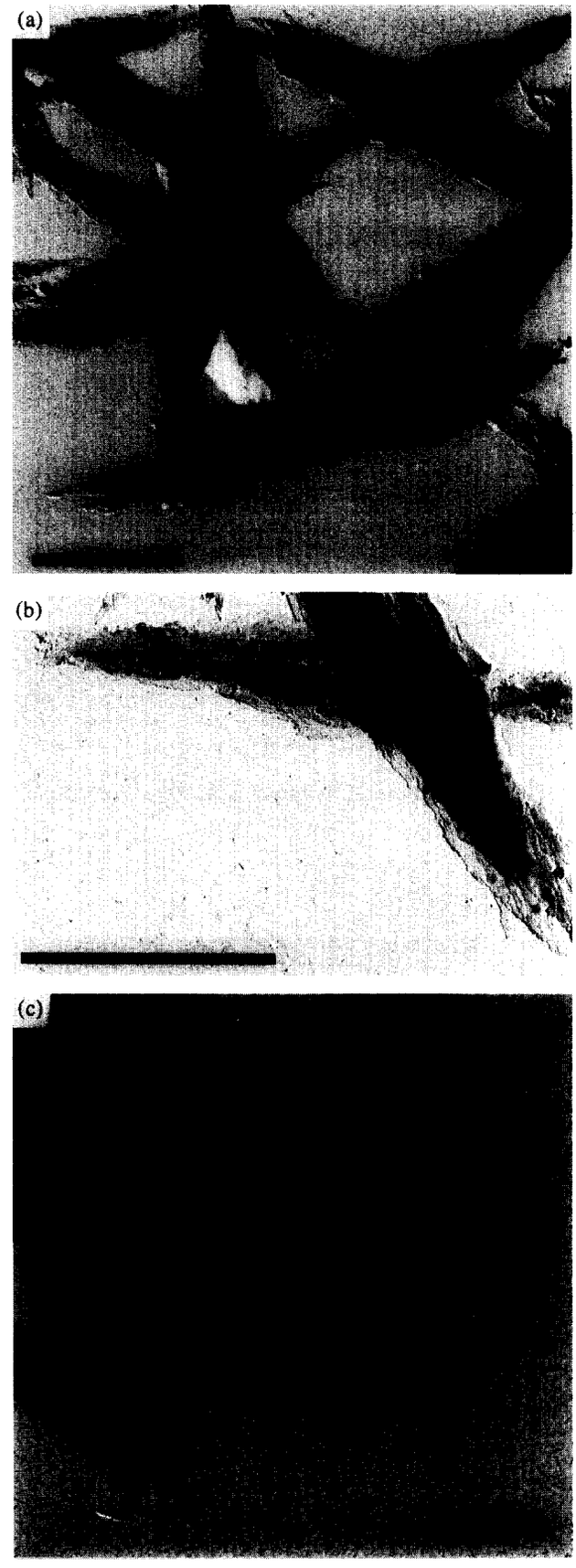


**Figure 2** Electron micrographs of PK99 solution grown single crystals. The scale bars represent 1 $\mu$m. (a) A typical group of multilayer crystals. (b) Lamellae seen at higher magnification, the multilayers are clearer, and the tendency to twist can be seen, particularly where there are many layers. (c) PK99 crystals decorated with polyethylene and shadowed with Pt/Pd, in accordance with the Wittmann and Lotz decoration technique[10], the polyethylene fibrils are randomly arranged on the carbon substrate, but line up on the crystal surfaces at right angles to the long directions of the crystals

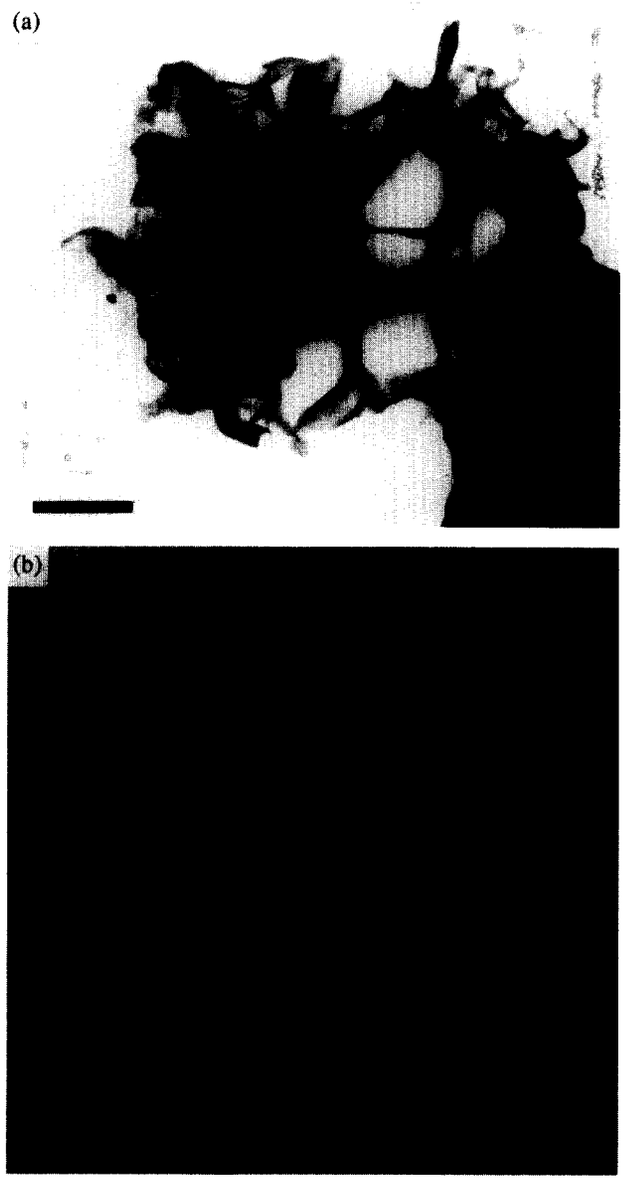


**Figure 3** Electron micrographs of spherulites of PK99. Scale bars represent 1 $\mu$m. (a) A group of crystals precipitated from 0.05% solution. In this low magnification picture the twisting of the lamellae is very obvious. (b) Spherulites grown in a thin film which had been melted and then held at 225°C for 4 min before quenching

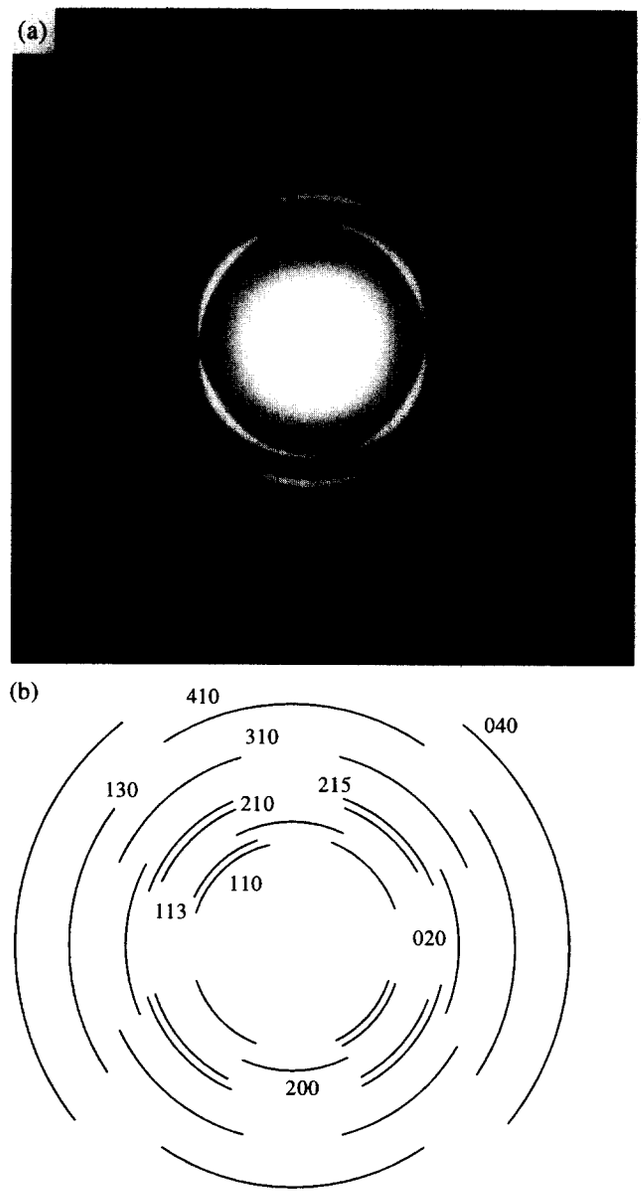


**Figure 4** (a) and (b) are in the same orientation. (a) Selected area electron diffraction pattern from a multilayer PK99 crystal (such as one of the leaf shaped entities seen in *Figure 2*). (b) Drawing to show signals are that observed by selected area electron diffraction. The indices are included, based on an orthorhombic unit cell with $a = 0.788$ nm, $b = 0.609$ nm and $c = 4.82$ nm

the same temperatures. Thin sections of PK99 were microtomed at room temperature, using an LKB microtome with a diamond knife. The sections, mounted on copper TEM grids (without carbon support film), were melted for 10 min in a Perkin Elmer DSC 2; cooled at 40°C min$^{-1}$ (DSC 2 cannot cool at 50°C min$^{-1}$) to the required crystallization temperature and held there for various lengths of time before quenching into acetone at freezing point. The quenched crystals were examined in the TEM and the growth rates measured from micrographs of quenched crystals.

The fibres were extruded from the melt, quenched into water and then annealed at 120°C; this process gave amorphous fibres. Each amorphous fibre was then mounted in a drawing frame and held in an oil bath at 200°C, where it was drawn, in a controlled way, to a draw ratio of about 1:4. This process yielded highly crystalline, well oriented fibres. X-ray patterns were obtained with the draw axis both parallel and perpendicular to the X-ray beam.

## RESULTS

### *Electron microscopy*

Typical PK99 solution grown lamellar single crystals are shown in *Figure 2*. Note that the crystals are elongated and usually multilayered. They grow in groups; we reduced the dilution and varied the crystallization temperature but we were unable to obtain individual crystals. PK99 crystals look very similar to those of PEEK and PEK (compare *Figure 2* with ref. 4, *Figures 2a* and *b*). Twisting about the long axis of the crystals is often evident, particularly where there are large crystal aggregates (for instance in the centre of the main crystal group in *Figure 2a*); crystals of PEEK and PEK also commonly twist about their long axes[4].

Wittmann and Lotz[10] have shown that, for a range of polymers, when polyethylene is evaporated onto the surfaces of lamellar crystals the evaporated material is ordered where the crystal surface is folded. The

**Table 1** Measured and calculated electron diffraction spacings $d$ (nm) for PK99

| Index[a] | | | | |
|---|---|---|---|---|
| *hk0* | *hkl* | Observed spacing ±0.002 nm | Calculated spacing ± 0.003 nm | Approx intensity[b] |
| 110 | | 0.486 | 0.482 | vs |
| | 113 | 0.468 | 0.462 | w |
| 200 | | 0.392 | 0.392 | s |
| 210 | | 0.330 | 0.330 | w |
| | 215 | 0.312 | 0.313 | m |
| 020 | | 0.309 | 0.305 | m |
| 310 | | 0.241 | 0.241 | w |
| 130 | | 0.197 | 0.197 | m |
| 410 | | 0.183 | 0.187 | w |
| 040 | | 0.152 | 0.152 | vw |

[a] On the basis of an orthorhombic unit cell with parameters: $a = 0.788$ nm, $b = 0.609$ nm, $c = 4.82$ nm
[b] Abbreviations denote relative intensities: vs = very strong, s = strong, m = medium, w = weak and vw = very weak

evaporated polyethylene builds up into small, elongated, rod-like, crystalline lamellae which are randomly distributed on carbon support film, and on the surfaces of crystals where there is no folding (e.g. crystals of unfolded paraffins), but are aligned on polymer fold surfaces, lying normal to the direction in which the chains fold[10]. PK99 crystals decorated with polyethylene are shown in *Figure 2b*. There is certainly ordering of the polyethylene on the crystal, particularly where individual layers are observed, the rods of evaporated polyethylene lie at right angles to the long dimensions of the crystals, indicating that the folds run parallel to this long direction. The ordering is not as pronounced as it is for crystals of polyethylene[11] but it is as good as that on the surfaces of lamellar crystals of nylons[12–14].

In some preparations it was possible to find spherulites as well as single crystals. The spherulitic material consists of groups of irregular ribbon-like lamellae, twisted together and growing form sheaf-like centres. *Figure 3a* shows a sheaf grown from solution, where large scale twisting of lamellae about their long axes is particularly clear. *Figure 3b* shows a spherulite growing in a thin film of PK99. The morphology of these spherulites is similar to those of a number of other polymers, for example nylon 6[15].

*Electron diffraction.* Electron diffraction proved relatively easy because PK99 (in common with PEEK and other polyaryls) is more stable in the electron beam than non-aromatic polymers. A typical electron diffraction pattern is shown in *Figure 4a*, the arced groups of multiple diffraction signals result from misorientation within the multilayer crystallites. The diffraction pattern is drawn out in *Figure 4b* (in the same orientation as *Figure 4*a) to indicate weaker reflections, barely visible in the print. Ten independent signals can be observed in many of the patterns. The signals are labelled in *Figure 4b* and listed in *Table 1*, together with the indices that we assign to each (on the basis of the unit cell that we propose, see below). The diffraction pattern is generally consistent with the *hk0* projection of an orthorhombic unit cell, indeed with that of Blundell *et al.*[3]. However, the several pairs of close reflections suggest that we do not have a pure *hk0* projection but that some *hkl* signals are present (as is the case for lamellar crystals of PEEK and PEK).

**Table 2** Unit cell dimensions, *hk0* projection

| Polymer | $a$ (nm) | $b$ (nm) |
|---|---|---|
| PK99 | 0.788 | 0.609 |
| PEEK[a] | 0.775 | 0.586 |
| PEK[a] | 0.763 | 0.596 |

[a] Data from ref. 4

Because PK99 has a large chain repeat, the spacings of *hkl* signals with the same *h* and *k* but differing *l* are very similar, so it is not possible to identify these unambiguously on the basis of spacing alone. For instance, there are two electron diffraction signals in the orientation expected for *211* signals, a strong signal measured at 0.312 nm and a weak signal at 0.330 nm. The calculated spacing of the *210* is 0.331 nm, that of the *215* is 0.313 nm, the *211* (0.330 nm), *212* (0.328 nm), *213* (0.324 nm), and *214* (0.319 nm) lie in between. The errors in measuring up the electron diffraction patterns give an uncertainty of ±0.003 nm and the errors in the cell parameters are ±0.002 nm, giving rise to further uncertainty. It is clear that the two signals observed come from the group *21l*, with *l* between *0* and *5*, but we cannot safely say, on the basis of measurement of the electron diffraction pattern, if we have *210* and *215*, or *211* and *215* or, possibly, some other pair. However, we have the X-ray pattern of the well-oriented fibre available for comparison. In this pattern the *l* index is unambiguous because the layer lines are clearly separated (see below). In the fibre pattern we see two *211* signals, a strong *215* signal and a weak *210* signal, so we believe that the two *211* signals appearing in the electron diffraction are *210* and *215*. On similar grounds we believe that the weak signal observed in the electron diffraction pattern just outside the *110* is the *113*.

The orientation of each crystal, with respect to its diffraction pattern, indicates that the crystals are elongated along the long axis, *b*. This is also the case in PEEK and PEK[4,8]. Crystals of PEEK and PEK are prone to twist about *b*, and show signals indexing as *111*, *311* and, particularly strongly, *211*, in many electron diffraction patterns[4]. In PK99 the *113* is seen, but it is the *215*, rather than the *211* that is prominent. Because the *c* repeat in PK99 is large, a relatively small twist is required to bring the strong *hkl*

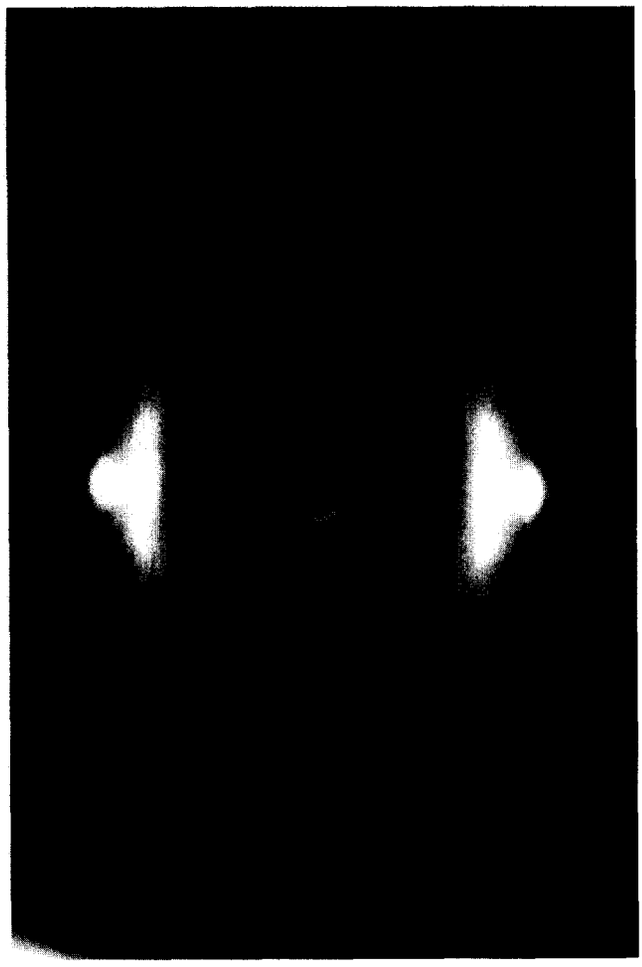

**Figure 5** Wide-angle X-ray pattern of a PK99 fibre, fibre axis vertical. The fibre is well oriented. Note the *1 1 0* and *2 0 0* strong on the equator, the *1 1 3* and *1 1 6* on the first row line (the *1 1 9* and *1 1 19* are clear on the negatives) and the *2 1 5* on the 5th layer line (noticeably lower than the 6th layer containing the *1 1 6*)

(The *c* spacing has been assessed from the X-ray fibre pattern, see below.) These values for the cell parameters are similar to those quoted by Blundell *et al.*[3]. The *a* and *b* parameters are larger than those of PEEK and PEK, as indicated in *Table 2*. We believe that *a* and *b* are larger for PK99 because the lattice has to expand to include the awkwardly shaped *meta* linkage within the crystal.

*Wide angle X-ray diffraction (WAXD).* The results can be best understood if the WAXD of the fibre is considered first.

*WAXD of the fibre*

A wide angle diffraction pattern obtained from a PK99 is shown in *Figure 5* and the signals are listed in *Table 3*. Other polymers from the family of poly(aryl ether ketone)s give very similar patterns[7,16,17]. The fibre is well oriented, so that the *l* index of each reflection can be determined unambiguously; the difference between the 6th (the *1 1 6* is visible) and the 5th (the *2 1 5* is visible) layer lines is quite clear and we can see a strong signal at 0.313 nm on the 5th layer line. This confirms that we were correct to assign the index *2 1 5* to the strong signal measured at 0.312 nm in the electron diffraction pattern; the position of the signal at 0.468 nm also confirms that the electron diffraction signal at this spacing is the *1 1 3*. Far out (on the original negatives) we can see a further strong signal, the *1 1 19* at 0.223 nm.

The spacings of the *h k 0* diffraction signals on the equator are in good agreement with the electron diffraction data. The even indexed *0 0 l* reflections, *0 0 2*, *0 0 4* and *0 0 6* are visible, indicating a two fold helix. Not all these *0 0 l* reflections are clear in the figure, others, listed in the table, can be seen on photographs taken at longer specimen to film distances.

*WAXD of the crystal mat*

WAXD pattern from a single crystal mat is shown in *Figure 6*. The orientation is poor and not simply that of stacked flat lamellar crystals. Because of the poor orientation of the crystal mat the signals have been indexed with reference to the electron diffraction pattern and to the WAXD pattern of the well-oriented fibre.

**Table 3** Measured and calculated X-ray diffraction spacings *d*(nm) for the fibre of PK99

| Index[a] *h k 0* | *h k l* | Calculated spacing ±0.002 nm | Observed spacing ±0.005 nm | Intensity[b] | Orientation[c] |
|---|---|---|---|---|---|
| | 0 0 2 | 2.410 | 2.410 | mw | M |
| | 0 0 4 | 1.205 | 1.210 | m | M |
| | 0 0 6 | 0.803 | 0.805 | mw | M |
| 1 1 0 | | 0.482 | 0.482 | vs | E |
| 2 0 0 | | 0.392 | 0.394 | vs | E |
| 2 1 0 | | 0.330 | ~0.32 | vvw | E |
| | 1 1 3 | 0.462 | 0.465 | vs | offM |
| | 1 1 6 | 0.413 | 0.417 | m | offM |
| | 1 1 9 | 0.358 | 0.361 | w | offM |
| | 1 1 19 | 0.224 | 0.222 | m | offM |
| | 2 1 5 | 0.313 | 0.313 | m | offM |

[a] On the basis of an orthorhombic unit cell with parameters: $a = 0.788$ nm, $b = 0.609$ nm, $c = 4.82$ nm

[b] Abbreviations denote relative intensities: vs = very strong, s = strong, m = medium, mw = medium weak, w = weak, vw = very weak and vvw = very very weak

[c] Abreviations denote relative orientation: M = meridional, E = equatorial, offM = off-meridional

signals into reflecting position. It was difficult, but possible, to find crystal tips and edges where only *h k 0* signals were visible (with no trace of *1 1 3* and *2 1 5*).

The unit cell that we propose for PK99 is orthorhombic, with $a = 0.788$ nm, $b = 0.609$ nm and $c = 4.82$ nm.

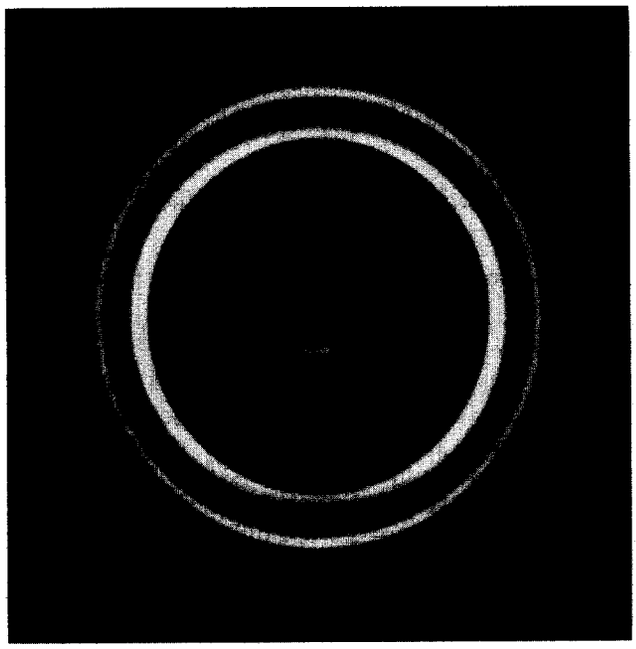

**Figure 6** Wide-angle X-ray diffraction pattern of a sedimented mat of PK99, mat normal vertical. The orientation in this pattern is poor, but some intensification can be seen on the equator of the innermost strong arc, *1 1 0*, and on the meridian of the second strong arc, *2 0 0*. This sort of pattern has been recorded in other polymers, where there are stacks of roughly two dimensional aggregates of twisted crystals (e.g. for polyethylene[18], PEEK and PEK[4])

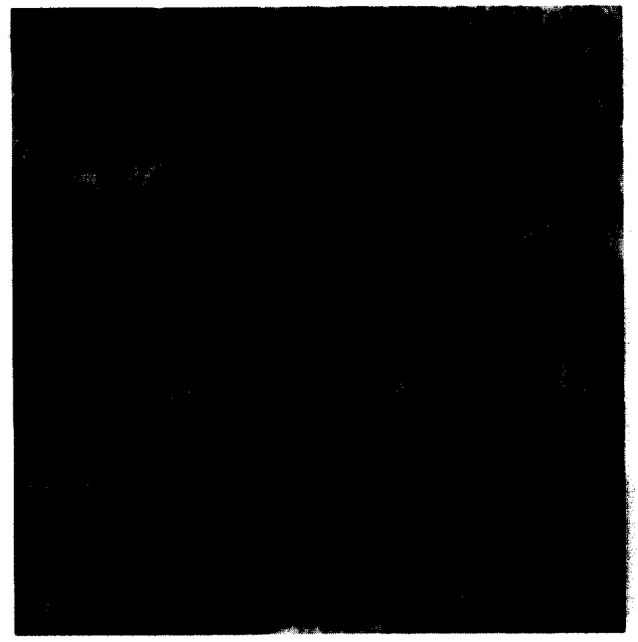

**Figure 7** Optical micrograph of PK99 spherulites. Crossed polars. This PK99 film had been held at 250°C for 15 min. The scale bar represents 30 $\mu$m

**Table 4** Measured and calculated X-ray diffraction spacings $d$(nm) for the MAT of PK99. The first two signals arise from the lamellar repeat and do not index on the unit cell

| Index[a] *h k 0* | Index[a] *h k l* | Calculated spacing nm ±0.002 nm | Observed spacing (nm) | Intensity[b] | Orientation[c] |
|---|---|---|---|---|---|
| SAXD | | 8.07 | 7.96 ± 0.08 | m | M |
| SAXD 2nd order | | Used to assess lamellar repeat | 4.035 ± 0.08 | m | M |
| | 0 0 2 | 2.41 | 2.4 ± 0.1 | m | M |
| ?? | ?? | | 1.56 ± 0.08 | m | E |
| ?? | ?? | | 1.33 ± 0.07 | m/w | E |
| | 0 0 4 | 1.204 | 1.16 ± 0.05 | m | M |
| | 0 0 6 | 0.803 | 0.82 ± 0.03 | m | M |
| ?? | ?? | | 0.71 ± 0.03 | m/w | M |
| | 0 0 8 | 0.602 | 0.609 ± 0.03 | m/w | M |
| | | Calculated ±0.002 nm | Observed ±0.005 nm | | |
| 1 1 0 | | 0.482 | 0.486 | vs | E |
| | 1 1 3 | 0.462 | 0.464 | s | |
| | 1 1 6 | 0.413 | 0.417 | m | |
| 2 0 0 | | 0.394 | 0.391 | vs | M |
| | 1 1 9 | 0.358 | 0.362 | mw | |
| | 2 1 5 | 0.313 | 0.312 | m | |
| 0 2 0 | | 0.305 | 0.307 | w | |
| 3 1 0 | | 0.241 | 0.242 | m | |
| | 1 1 19 | 0.224 | 0.223 | m | |
| 1 3 0 | | 0.197 | 0.196 | m | |

[a] On the basis of an orthorhombic unit cell with parameters: $a = 0.788$ nm, $b = 0.609$ nm, $c = 4.82$ nm
[b] Abbreviations denote relative intensities: vs = very strong, s = strong, m = medium, w = weak and vw = very weak
[c] Abreviations denote relative orientation: M = meridional, E = equatorial

Strong signals at the same characteristic spacings are consistently seen in electron diffraction of single crystals (*Table 1*) and in WAXD from the fibre (*Table 3*) and from the mat (*Table 4*). The WAXD pattern of the mat is typical of a 'row structure' composed of a stack of discs made up of twisted ribbons; such morphologies were first studied in polyethylene[18], and have also been observed in PEEK and PEK[4]. The appearance of a

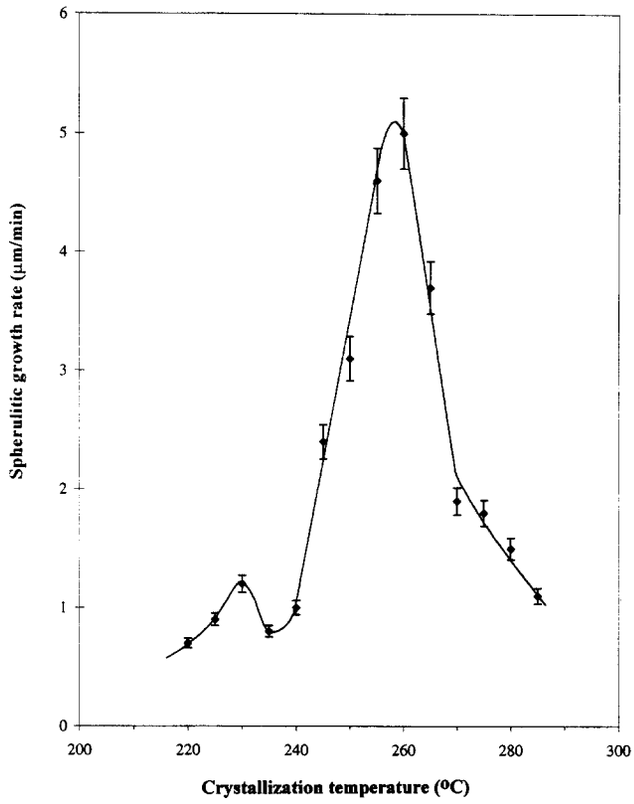


**Figure 8** Variation of growth rate with crystallization temperature in melt crystallized PK99. The figure shows the growth rates measured over the first 10 min of growth. The observational errors are indicated

maximum in intensity of the 200 on the meridian is characteristic of row structures in these polymers with orthorhombic unit cells, where the chain folded lamellae twist about *b*.

*Table 4* lists the X-ray data for the single crystal mat. A number of *00l* signals (for even *l*) are seen on the meridian of the diffraction pattern of the mat. Because of the large *c* repeat these signals are at large spacings and they are all weak, so errors of measurement are larger than for the WAXD signals at smaller spacings. There are three faint signals, visible in the WAXD pattern of the crystal mat but not found in the WAXD pattern of the fibre or in the electron diffraction pattern. These signals, at 1.56, 1.33 and 0.71 nm, cannot be indexed on the basis of our unit cell.

*Small angle X-ray diffraction.* Small angle X-ray diffraction (SAXD) of the crystal mat revealed a low angle period of 7.86 nm, only the first and second orders of the low angle appear, indicating rather poor lamellar stacking, as we can deduce from the WAXD pattern. The SAXD signals are listed in *Table 4*, together with the WAXD signals from the mat.

The small angle spacing of PK99 crystallized from the melt at both 230 and 260°C was 14.8 nm. This should be compared with the value of 13.6 nm found by Blundell *et al.*[3] for material crystallized at 260°C. Blundell *et al.* recorded a smaller spacing (11.9 nm) after crystallization at 230°C.

*Crystal growth rates—optical microscopy and TEM*

A typical optical micrograph of PK99 spherulites is shown in *Figure 7*. These particular spherulites grew at 250°C. An electron micrograph showing younger spherulites is shown in *Figure 3b*; in this case the film was quenched after crystallization for 4 min at 225°C.

*Figure 8* shows the variation of growth rate with crystallization temperature, there is a maximum growth rate at 260°C, a minimum between 235 and 240°C and a second, much lower, maximum at 230°C. These growth rates were measured over a 10 min period. Results from TEM agree with those from OM within the experimental errors. The maximum growth rate, at 260°C, is 5 $\mu$ min$^{-1}$ for our material.

## DISCUSSION

It is clear that single crystals of PK99, grown from solution, are very like those of PEEK and PEK[4,8]. All three materials dissolve in benzophenone, crystallize to give similar looking multilayer crystals and all have orthorhombic unit cells. A unit cell with $a = 0.788$ nm, $b = 0.609$ nm and $c = 4.82$ nm, containing two chains, is consistent with our data for PK99. The values of *a* and *b* are similar in all three polymers, although *b* is some 5% larger for PK99 than for PEEK or PEK, perhaps because of the difficulty in including the awkwardly shaped *meta* linkage within the crystal. The crystals are elongated along *b* in all three polymers and there is a strong tendency for the crystals to twist about this direction, as a result certain *h k l* signals usually appear in electron diffraction patterns of crystal aggregates and the WAXD pattern of the PK99 mat is that of a 'row structure'. In PEEK and PEK the *2 1 1* signals are especially strong, but in PK99 it is the *2 1 5* that is prominent; Blundell[7] mentions a proposed structure for PK99 that would give clear *2 1 5* signals, as we observe, but he does not give a complete list of all expected signals or a table of expected intensities.

The Wittmann and Lotz decoration technique[10] shows that lamellar crystals of PK99 have quite well ordered fold surfaces, and that the chains run along the long direction of the crystals. The latter is as expected; chains usually run in this direction for elongated crystals of this shape[12–14,19] and this is the case for both PEEK and PEK[4,8]. It is not, however, a foregone conclusion that PK99 will have a well-ordered fold surface. The chain must be quite stiff, because of the bulky aromatic groups. Folding will not be easy, and we might expect loops, or stiffer spikes of chain, sticking out of the fold surface. Further, there may be some difficulty in including the *meta* group within the crystal, a problem which could lead to additional irregularity within the fold surface (this is discussed in refs 2 and 3). However, *Figure 2b* shows that there is a reasonable degree of overall order in the fold surface of solution grown PK99 crystals in spite of these possible hindrances to crystallinity. The SAX spacing of the single crystal mat, at 7.86 nm, is typical of solution crystallized polymers but, because of the very long chain repeat, PK99 is unusual in that the SAX spacing is only just over one and a half times the chain repeat.

The electron diffraction and the WAXD patterns from the single crystal mat and from the fibre are consistent with each other, apart from the additional signals seen in the mat pattern at 1.56, 1.33 and 0.71 nm. The indexing of these signals is problematic; the signal at 0.71 nm could possibly be the *0 0 7* (calculated spacing 0.69 nm),

but the *0 0 7* is absent from the fibre pattern (as are other *0 0 l* signals for odd *l*) and we would not expect to see it in the mat pattern where the spread of the *0 0 l* signals is greater. Since the anomalous signals appear in the WAXD pattern of the mat, but not in the fibre patterns, we believe that they do not come from the crystallographic cell itself. Signals that could not be indexed on a proposed unit cell have arisen in simulated X-ray diffraction patterns computed for chain folded proteins[20,21]. The extra signals in the simulated protein patterns were shown to arise from diffraction of the folds, which were not constrained to the same symmetry as the straight stems in the crystal core. The extra signals observed in the present case, for mats of PK99 lamellae, could result from a similar cause, particularly as the rigid phenol rings will restrict the number of possible fold conformations, so that the fold surface can not be treated as a simple amorphous region. Detailed computer modelling would be required to clarify this point. In the context of further modelling, it has not escaped our notice that the *1 1 19* signal is prominent in the diffraction pattern of the mat and of the fibre. This will be useful in detailed crystal structure analysis in deciding on the setting angle of the chains and in consideration of the *c* axis relationship between the two chains in the cell.

There is a maximum in the growth rate of PK99 on crystallization from the melt at 260°C, a minimum between 235 and 240°C and a second, much lower, maximum at 230°C. The measurements of growth rates by OM and by TEM were in agreement with each other within the experimental errors. The existence of the double maximum in growth rate confirms previous work by Liggat *et al.*[2,3]. They found a higher maximum at 270°C and a minimum at 245°C; their lower maximum was at 230°C, as is ours. The actual growth rates are similar in the two sets of experiments, the maximum growth rate for their material is $3.5\,\mu\,min^{-1}$, and the maximum for ours $5\,\mu\,min^{-1}$. The maximum growth rate for our material was obtained from measurements up to 10 min. At longer times the growth rate gradually reduced; changes in crystal growth rate have been recorded previously in other polymers, and attributed to the presence of impurities[22,23], the presence of irregularities in some polymer chains[22,23] or to differences in molecular weight, for instance as a result of degradation[24]. The average growth rate measured over 20 min is $3.7\,\mu\,min^{-1}$ for our material. Liggat *et al.* do not state the time scale of their experiment.

Since the materials used in the two sets of experiments were synthesized at different times and places it is likely that the molecular weights and molecular weight distributions of the two batches of polymer are different. There is a similarity in behaviour between the two samples (double maxima) but slightly different values are recorded for the peak temperatures. This indicates that the unusual growth rate pattern is not unique to one particular batch of polymer or molecular weight, but may be general for this material. Liggat *et al.*[2,3] suggest that the reason for the variations in growth rate could be associated with the matching between molecular sequence length and lamellar thickness.

Blundell *et al.* found that crystals of all thicknesses had the same structure; in addition we now find that both solution grown lamellae and melt crystallized fibres have the same structure as melt crystallized PK99. Our values for SAXD maxima from melt crystallized material are similar to those of Blundell *et al.*, but, unlike those authors, we did not find any difference between the SAXD spacings of material crystallized from the melt above and below the temperature of minimum growth rate. In the light of this, it is not obvious that Liggat *et al.*'s explanation for the double minimum in growth rate would be applicable to our samples.

## CONCLUSIONS

(a) Single crystals of PK99 can be grown from solution in the solvent benzophenone.

(b) The PK99 crystals are elongated, lath shaped and usually multilayer. They have a strong tendency to twist about the direction of elongation. In these respects they are very like the solution grown crystals of PEEK and PEK.

(c) The crystals are orthorhombic, as are those of PEEK and PEK. The unit cell consistent with our data (from isolated single crystals, crystal mats and fibres) has $a = 0.788$ nm, $b = 0.609$ nm and $c = 4.82$ nm. The cell is close to that determined by Blundell *et al.*[3] who examined melt crystallized material. The crystals are elongated along *b*.

(d) The crystal structure of PK99 is similar to that of PEEK and PEK in *h k 0* projection. It is, however, slightly larger, probably because of the extra space required to include the awkwardly shaped *meta* linkage in the chain. In the diffraction patterns of crystal aggregates of PEEK and PEK the 2 1 1 reflection is prominent; in PK99 it is the 2 1 5 that is strong.

(e) The SAXD spacing from the single crystal mat is 7.86 nm, only about one and a half times the chain repeat (4.82 nm).

(f) When PK99 (from the batch we used) is grown from the melt there is a growth rate maximum at 260°C, a minimum between 235 and 240°C and a second maximum, much lower than the first, at 230°C.

## ACKNOWLEDGEMENTS

L. F. acknowledges financial support from the EU through a grant from the Human Capital Mobility program. M. B. thanks Prof. A. Recca and the University of Catania for support and for leave of absence to work in Bristol. We are grateful to Prof. E. D. T. Atkins and Dr S. J. Cooper for very helpful discussions.

## REFERENCES

1. Staniland, P. A., Wilde, C. J., Bottino, F. A., Di Pasquale, G. and Recca, A., *Polymer*, 1992, **33,** 1976.
2. Liggat, J. J. and Staniland, P. A., *Polymer Communications*, 1991, **32,** 450.
3. Blundell, D. J., Liggat, J. J. and Flory,A., *Polymer*, 1992, **33,** 2475.
4. Waddon, A. J., Hill, M. J., Keller, A. and Blundell, D. J., *J. Mater. Sci.*, 1987, **22,** 1773.
5. Ungar, G. and Keller, A., *Polymer*, 1987, **28,** 1899.
6. Cheng, S. Z. D. and Chen, J., *J. Polym. Sci. Polym. Phys.*, 1991, **29,** 311.
7. Blundell, D. J., *Polymer*, 1992, **33,** 3773.
8. Lovinger, A. J. and Davis, D. D., *Polymer Communications*, 1985, **26,** 322.

9. Bellomo, M., Ph.D. thesis, University of Catania, Sicily, 1996.
10. Wittmann, J. C. and Lotz, B., *J. Polym. Sci., Polym. Phys.*, 1985, **23,** 200.
11. Organ, S. J. and Keller, A., *J. Polym. Sci.*, 1987, **B25**, 2409.
12. Atkins, E. D. T., Hill, M. J., Hong, S. K., Keller, A. and Organ, S. J., *Macromolecules*, 1992, **25,** 917.
13. Jones, N. A., Atkins, E. D. T., Hill, M. J., Cooper, S. J. and Franco, L., *Macromolecules*, 1996, **29,** 6011.
14. Jones, N. A., Atkins, E. D. T., Hill, M. J., Cooper, S. J. and Franco, L., *Polymer*, 1997, **38**, 2689.
15. Geil, H. P., *Polymer Single Crystals*. Interscience Publishers, 1963.
16. Dawson, P. C. and Blundell, D. J., *Polymer*, 1980, **21,** 577.
17. Blundell, D. J. and Newton, A. B., *Polymer*, 1991, **32,** 308.
18. Machin, M. J. and Keller, A., *J. Macromol. Sci. (Phys).*, 1967, **B1,** 41.
19. Barham, P. J., Keller, A., Otun, E. L. and Holmes, P. A., *J. Mater. Sci.*, 1984, **19,** 2781.
20. Krechi, M. T., Deguchi, Y., Fournier, M. J., Mason, T. L., Tirrel, D. A., Cooper, S. J. and Atkins, E. D. T., Submitted to *Macromolecules*.
21. Panitch, A., Matsuki, K., Cantor, E. J., Cooper, S. J., Atkins, E. D. T., Fournier, M. J., Mason, T. L. and Tirrel, D. A., *Macromolecules*, 1997, **30**, 42.
22. Keith, H. K. and Padden, F. J. Jr., *J. Appl. Phys.*, 1964, **35,** 1270.
23. Keith, H. K. and Padden, F. J. Jr., *J. Appl. Phys.*, 1964, **35,** 1286.
24. Suzuki, T. and Kovacs, A., *Polym. J.*, 1970, **1,** 82.